# Shepherd Nova

## A Public Testbed for Rigorous Experiments Under Repeatable Energy-Harvesting Conditions

Geissdoerfer, Kai; Splitt, Ingmar; Sokolowski, Matthias; Herrmann, Carsten; Kubicki, Jonas; De Winkel, Jasper; Zimmerling, Marco

**DOI**
10.1145/3711875.3729146



**Publication date**
2025

**Document Version**
Final published version

**Published in**
MobiSys 2025 - Proceedings of the 23rd ACM international Conference on Mobile Systems, Applications, and Services

Geotech Geol Eng (2025) 43:485
https://doi.org/10.1007/s10706-025-03446-y

ORIGINAL PAPER

# Full-Scale Surcharge Test on Softwood Timber Sheet Pile Walls for Sustainable Canal Embankments

**Abhijith Kamath · Giorgos Stamoulis · Wolfgang Gard · Jan-willem van de Kuilen**

Received: 13 May 2025 / Accepted: 11 September 2025


**Abstract** Traditional "hard" protection systems, such as hardwood timber sheet pile walls, are often used to protect banks of canals and streams, but the tropical hardwood they require is not always locally available. This has led to increasing interest in nature-based, bio-engineered solutions that combine locally sourced wood with vegetation to protect the soil. To assess the behaviour of locally available softwood timber sheet pile walls, a full-scale surcharge loading test was performed under realistic conditions. The test applied a 30 kPa surcharge load, representing the weight of a heavy agriculture machinery, while monitoring the wall's horizontal and vertical displacement, along with its rotation at the top, mid-height, and base of the retained soil. This resulted in a displacement of approximately 1.9% of the one meter retaining height. The potential onset of a failure wedge was observed after an extended loading period. Nonlinear tilt measurements showed peak curvature at mid-depth (0.66° top, 0.71° mid, 0.69° bottom), indicating dominant flexural bending. Additionally, the measured horizontal displacement exceeded the rotational contribution estimated from the tilt. The material properties of the softwood sheet piles were determined through four-point bending tests. A numerical model, calibrated with experimental data, was then developed to simulate the long-term performance (10 years) of decayed sheet piles with both bare and vegetated backfill. The results indicate that vegetated backfills significantly reduce displacement and the bending moment on the wooden sheet pile compared to bare soil.

**Keywords** Bio based retaining structure · Canal embankment · Vegetation reinforcement · Earth pressure

**Abbreviations**

| | |
|---|---|
| DC | Durability class |
| IBC | Intermediate Bulk Container |
| LSV | Soil laser sensor vertical |
| T1, T2, …, T10 | Tilimeter 1, Tilimeter 2, …, Tilimeter 10 |
| H1, H2, …, H6 | Horizontal laser sensor 1, …, Horizontal laser sensor 6 |
| V1, V2, V3, V4 | Vertical laser sensor 1, …, Vertical laser sensor 4 |
| $MOE_{s,g}$ | Global modulus of elasticity (MPa) |

**Supplementary Information** The online version contains supplementary material available at https://doi.org/10.1007/s10706-025-03446-y.

A. Kamath (✉) · G. Stamoulis · W. Gard · J. van de Kuilen
Department of Engineering Structures, Biobased Structures and Materials Group, Delft University of Technology, Stevinweg 1, 2628 CN Delft, The Netherlands
e-mail: A.C.Kamath@tudelft.nl

J. van de Kuilen
Wood Technology, Technical University of Munich, Winzererstrasse 45, 80797 Munich, Germany

Published online: 31 October 2025

| | |
|---|---|
| MOR | Bending strength (MPa) |
| $V$ | Velocity of the wave in vibration measurement (m/s) |
| $L$ | Length of the board (m) |
| $f$ | The first natural frequency (Hz) |
| MOEdyn | Dynamic modulus of elasticity (MPa) |
| *rho* | Density (kg/m$^3$) |
| MC | Moisture content (%) |
| F1 | Future scenario 1 |
| F2 | Future scenario 2 |
| F3 | Future scenario 3 |
| $MOE_{s,g12}$ | Global modulus of elasticity at reference Moisture content 12% (MPa) |
| $MOE_{s,l}$ | Local modulus of elasticity (MPa) |
| $\phi$ | Soil friction angle (degree) |
| EI | Elastic stiffness (kNm$^2$/m′) |

## 1 Introduction

The maintenance and restoration of canal and stream banks hold significant ecological, economic, cultural, and heritage value. Within the Netherlands alone, extensive lengths of canal embankments, potentially spanning hundreds of kilometres, are scheduled for maintenance or replacement within the coming decade, highlighting the scale of this challenge.

Traditionally, bank protection has relied on 'hard' engineering approaches, including timber or steel sheet piling, rock rip-rap, and even recycled plastic structures (Bigham et al. 2020). Sheet piles made of materials such as glass fiber reinforced plastics have also being studied for use in water front structures including streams and creeks (Li et al. 2021). However, a growing emphasis on environmental sustainability has spurred demand for bio-based and nature-friendly alternatives. These 'soft' or bio-engineering techniques are not novel; indeed, early forms of bank protection utilized organic materials such as living plants and cuttings alongside inert, locally sourced wood (Evette et al. 2009). In recent decades, these century-old principles have been revisited, with renewed efforts to develop formalized design methodologies for bio-engineering solutions (Pollen-Bankhead and Simon 2010; Guo et al. 2019; Jiang et al. 2022).

Vegetated crib walls exemplify such bio-engineered solution suitable for stabilizing soil slopes and banks (Gray and Sotir 1996; Tardío and Mickovski 2016; Acharya 2018). These structures typically integrate inert materials, like locally available wood, with living vegetation. The design philosophy relies on a phased approach (Tardío and Mickovski 2016; Mickovski et al. 2024): initially (Stage 1), the inert material provides primary bank protection. As this material, particularly wood, naturally degrades over time, a gradual load transfer occurs to the developing root systems of the vegetation (Stage 2). Ultimately (Stage 3), upon significant or complete decay of the inert components, the established vegetation is intended to provide long-term, self-sustaining bank stability.

This approach is currently studied and implemented worldwide, primarily due to its additional ecological benefits (Böll et al. 2009; Krymer and Robert 2014; Stokes et al. 2014; Fernandes and Guiomar 2016; Hubble et al. 2017; Zhang et al. 2018; Tardío and Mickovski 2023; Mickovski et al. 2024). Zhang et al. (2018) evaluated various structural forms of bio-engineered streambank protections, each comprising different numbers of rows of pine timber piles, riprap, and willow cuttings. The durability of the wooden structures was quantified by measuring the percentage of tilted timber piles during service period. A 'warning' value for maintenance was recommended at seven years, specifically when 33.3% of the piles had tilted. In a separate study, Mickovski et al. (2024) validated the design methodology discussed above by conducting a practical case study on an existing long crib wall.

The presence of vegetation contributes to stability of banks by providing additional soil reinforcement through root systems. The influence of root reinforcement is typically confined to the soil's upper layers, as generally majority of the roots are concentrated on the top layers of soil (Zhang et al. 2018; Andreoli et al. 2020). While the hydraulic and mechanical contributions of vegetation have been extensively researched (e.g., Ali and Osman 2008; Ni et al. 2018; Dias 2019; Li et al. 2024), the role of the inert components, particularly locally sourced softwood, and the synergistic effects within the wood-vegetation system warrant further investigation.

In the Netherlands, timber sheet piling is a common method for protecting canal banks. Current

practices often rely on imported tropical hardwood like Azobé (*Lophira alata* Banks ex C.F.Gaertn.), also known as Ekki (Van de Kuilen and Blaß 2005), or chemically treated Pine (*Pinus sylvestris* L.). The use of imported hardwood raises sustainability concerns due to transportation impacts and potential sourcing issues, as the Netherlands and neighbouring regions lack exploitable native hardwood forests suitable for this purpose. Treated pine, while potentially locally sourced, poses environmental risks associated with preservation chemicals. Consequently, even timber, a 'natural' material, becomes less environmentally favourable if not sourced locally and sustainably without aggressive treatment.

An alternative is locally available untreated softwood, such as Spruce (*Picea abies* (L.) H. Karst.). Widely used in Dutch construction for its availability and cost-effectiveness, Spruce offers a potential local resource for bank protection. However, its natural durability is considerably lower than tropical hardwoods; its heartwood is classified as Durability Class 4 (DC 4) according to EN 350: 2016 (on a scale where DC 5 is least resistant and DC 1 most resistant). Its expected service life in ground contact applications is significantly less than durable hardwoods such as Azobé and is estimated to be between 5 and 20 years.

Notably, the uppermost section of the wooden sheet pile, generally within the top 50 cm and situated at the air–water-soil interface, is susceptible to greater deterioration. Conversely, the submerged portion of the sheet pile demonstrates higher durability. Furthermore, as mentioned previously, vegetation roots developing in this upper, decaying section during stage 2 can potentially improve bank stability.

Employing locally sourced Spruce for sheet piling, especially when integrated with vegetation, aligns with bio-engineered solutions for bank protection. This research examines the viability of this approach using a combined experimental and numerical methodology. A full-scale, in-situ experiment was performed on a Spruce timber cantilever sheet pile wall, subjecting it to surcharge loading and measuring wall displacements, tilt, and soil settlement.

The experimental data obtained was used to calibrate a numerical model developed in D-Sheet Piling (Deltares 2024). Subsequently, the calibrated model was utilized to explore the potential effects of vegetation establishment on the deformation behavior and bending moments within the sheet pile wall.

## 2 Materials and Methods

### 2.1 Location and Soil Conditions

The surcharge loading test was conducted near Middenmeer, Province of Noord Holland, the Netherlands (52°48′07.8″N, 4°59′50.8″E). This test section is part of a larger, 100-m canal bank testing program. Preliminary field soil investigations were performed to a depth of 2.8 m. Soil cores were extracted using Ackerman samplers at 0.4-m intervals. Seashells were observed in all cores below a depth of 0.4 m. Visual inspection indicated that the soil consisted primarily of fine sand. A representative soil sample, encompassing the top 1.2 m, was oven-dried at 105 °C and subjected to dry sieve analysis.

The soil was classified as poorly graded sand according to the Unified Soil Classification System. The groundwater table was located between 1.0 and 1.2 m below the ground surface. Wet density measurements were conducted at various depths (Table 1). The uppermost 200 mm layer was found to be generally organic. The soil stratigraphy is illustrated in Fig. 1. Direct shear tests were performed on soil samples compacted to a density of 16 kN/m$^3$, resulting in a friction angle of 40°.

### 2.2 Site Preparation

The test section was situated a few meters behind an existing canal and sheet pile bank protection. The

**Table 1** Wet and dry density of soil with depth at test site

| Depth (cm) | Wet density (kN/m$^3$) | Dry density (kN/m$^3$) |
|---|---|---|
| 0–40 | 16.1 | 12.3 |
| 40–80 | 16.6 | 15.2 |
| 80–120 | 17.4 | 14.8 |
| 120–160 | 21.1 | 17.5 |
| 160–200 | 21.1 | 16.2 |
| 200–240 | 21.7 | 16.8 |
| 240–280 | 21.0 | 16.5 |

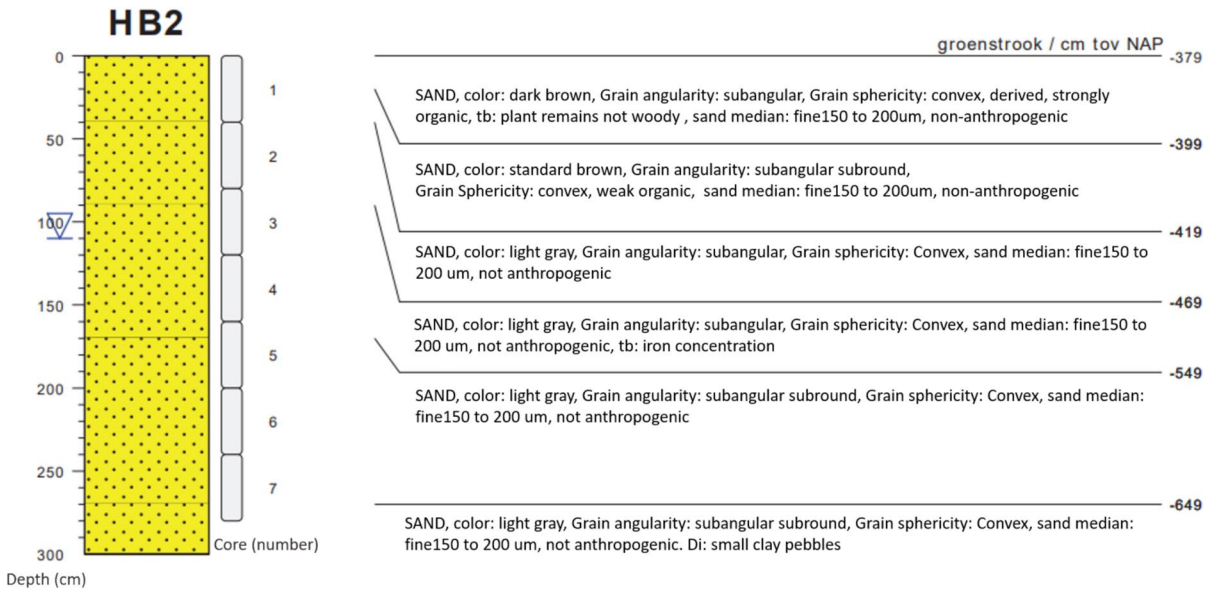


**Fig. 1** Soil stratigraphy at test site

original slope profile was approximately 1:3 (vertical: horizontal). A spruce cantilever sheet pile, 65 mm thick and 2.3 m in total length, was installed along a 7-m running length (Fig. 2). Approximately 0.3 m of soil was excavated from the front of the sheet pile and used as backfill. The topsoil and underlying fine sand were excavated and stockpiled separately. The backfilling process was conducted in layers, ensuring that the excavated topsoil was placed on top of the fine sand. To minimize lateral movement of the sheet pile edges during testing, a 0.3-m soil buffer was left undisturbed at each end of the sheet pile installation.

The sheet piles were interconnected using a tongue-and-groove joint. Horizontal timber members, measuring 67 mm × 40 mm, were placed along the top of the sheet pile for its entire running length. This site preparation resulted in a sheet pile height of 0.9 m above the levelled ground surface. The backfill surface was, on average, 0.1 m below the top of the sheet pile after preparation. The site preparation was completed in October 2022.

## 2.3 Testing Procedure

The full-scale test was performed during the last week of March 2023, approximately six months after the initial site preparation. In the period preceding and during the test days, soil moisture conditions were monitored using tensiometers and water content sensors previously installed to a depth of one meter in an adjacent plot situated approximately 15 m from the test structure, confirming near-saturated conditions.

Test procedures commenced with the installation of sensors (Sect. 2.4) to monitor horizontal and vertical displacements of the sheet pile. Tiltmeters T1 through T8 were also affixed to the structure at this stage, and initial zero readings were recorded for all instrumentation. Subsequently, the soil surface in front of the sheet pile was excavated to establish a precise exposed wall height of 1.0 m above the base level (elevation − 5.12 m, see Fig. 3), requiring the removal of approximately 0.1 m of soil on average. Following excavation, tiltmeters T9 and T10 were installed.

After allowing sufficient time for the initial horizontal displacements induced by the excavation to stabilize, the area behind the sheet pile was backfilled to create a retained soil height of 1.0 m. This involved adding an average soil layer thickness of 0.1 m along the structure's length. The backfill material was carefully tamped and levelled to ensure uniformity.

Once the structure's horizontal movement stabilized following the backfilling process, the saturation phase was initiated. Although data from the nearby monitoring plot indicated that the soil profile was already near saturation down to 1 m depth

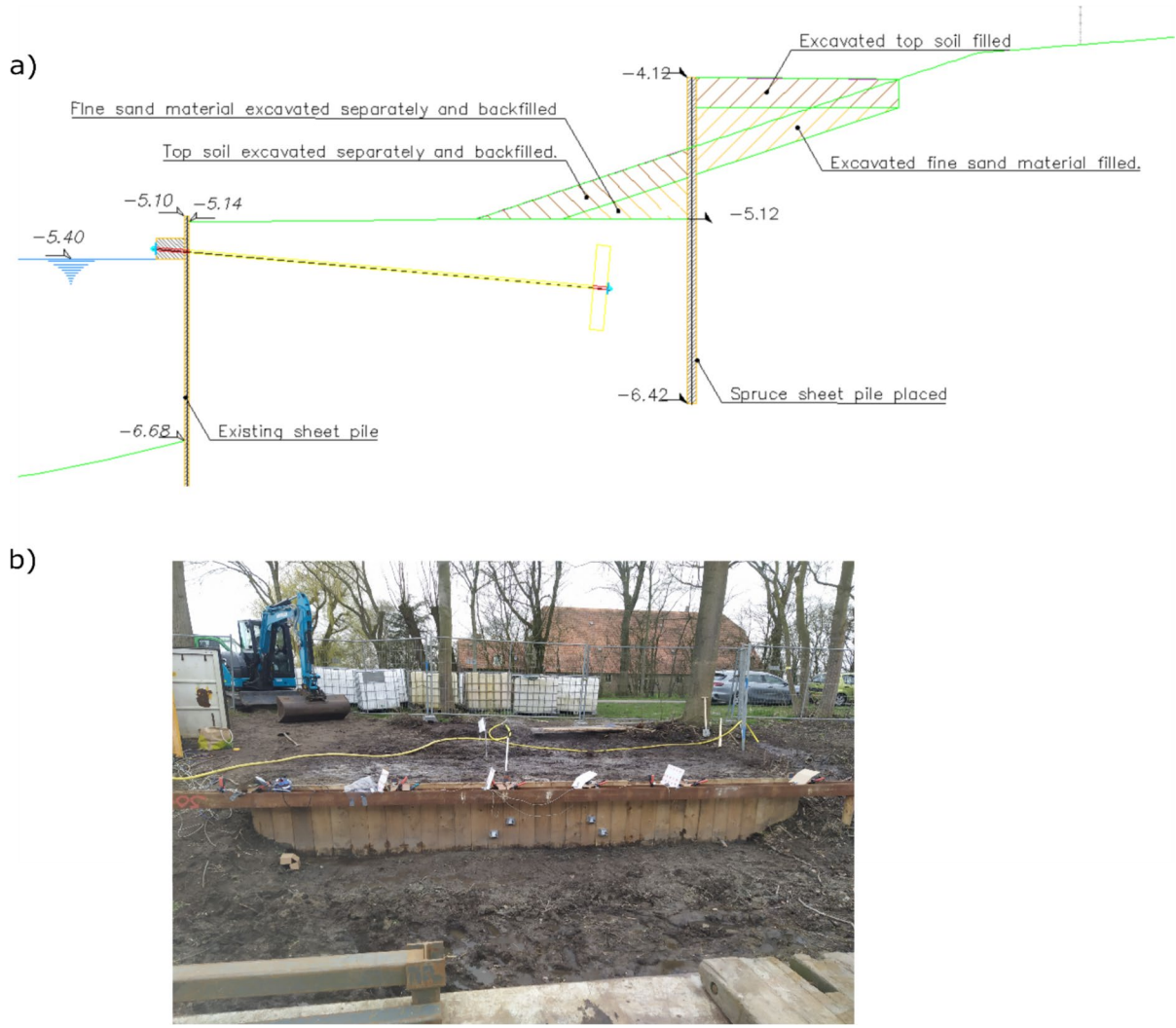


**Fig. 2** **a** Illustration of site preparation, excavation and backfilling before surcharge loading experiment, **b** Picture from the test site at the end of site preparation

(tensiometer readings close to zero water potential), artificial rainfall was applied to the backfill surface for three hours using a commercial sprinkler system to ensure thoroughly saturated conditions at the surface. The application was periodically paused when surface ponding occurred and resumed once the water infiltrated. Following the simulated rainfall, the entire test setup was left undisturbed overnight (approximately 16 h) to allow for pore water pressure equalization and further system stabilization before proceeding to the loading stage.

Prior to initiating the surcharge loading, a laser sensor was positioned to measure vertical settlement of the backfill surface. The surcharge load was applied incrementally using a stepped loading procedure. To ensure uniform load distribution over the 4.0 m long × 1.0 m wide area of backfill behind the sheet pile, a steel plate with corresponding dimensions (4.0 m × 1.0 m) was placed on the levelled ground surface. The load was generated by Intermediate Bulk Container (IBC) water tanks, each with a volume of 1 $m^3$. These tanks were positioned on the steel plate and filled sequentially with water pumped from the adjacent canal. The tanks were arranged in three layers, with four tanks per layer. For safety, each layer of tanks was secured

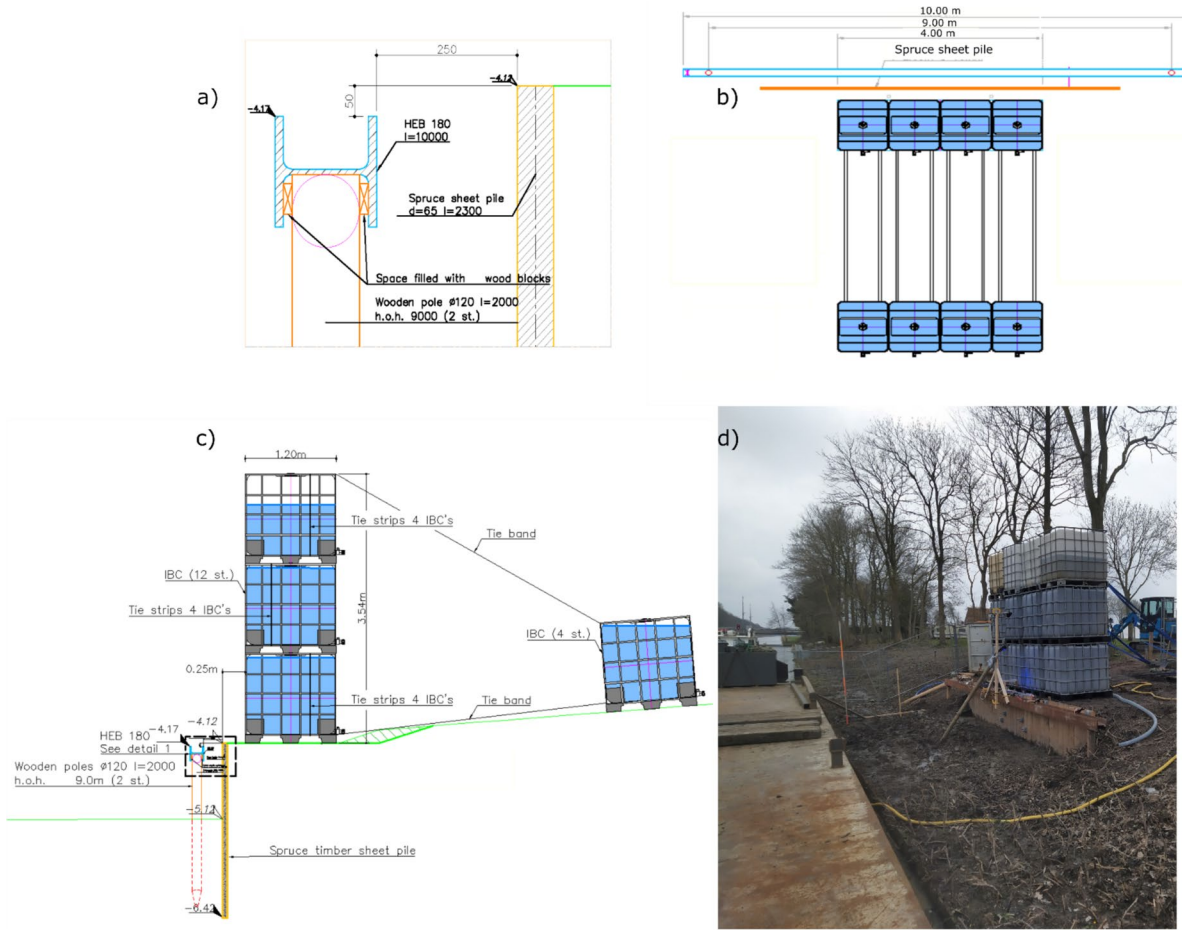


**Fig. 3** Loading setup **a** Detailing in the placing of HEB 180 beam, **b** Plan view of the test section **c** Testing setup section view, **d** Picture from the test site during surcharge loading

with tie ropes anchored to poles or water tanks fixed in the ground several meters behind the test area to prevent toppling in case of excessive deformation or failure.

A total of seven load steps were applied, corresponding to surcharge pressures of approximately 2, 5, 10, 15, 20, 25, and 30 kPa. The magnitude and duration of these steps were determined based on real-time monitoring of the structural response, logistical constraints aiming for test completion within approximately 24 h, and safety considerations. The maximum applied surcharge load was limited to 30 kPa which is representative of the typical maximum load expected from heavy agricultural machinery such as a large farm tractor, on an agricultural canal embankment. For safety, surcharge loading was stopped at this limit to mitigate the risk of container toppling in the event of a failure. Each load increment, from the completion of the previous step to reaching the target pressure of the next, typically took approximately 20 min to apply. The final load step of 30 kPa was maintained for a monitoring period of 16 h.

## 2.4 Sensors

To accurately measure sheet pile displacement, a stable reference frame was essential. A 9-m long HEB180 steel beam was used to create this reference frame, spanning the sheet pile's running length and extending beyond the test area (Fig. 3). The beam was supported by wooden poles positioned one

meter outside each end of the sheet pile. The poles supported the beam's web, with the flange oriented towards the sheet pile. The top of the beam was positioned 50 mm below the top of the sheet pile, and the beam was located 250 mm horizontally from the sheet pile.

Laser triangulation sensors (FDFR603 series) were used for all displacement measurements. The sensors were mounted on wooden blocks, which were then clamped onto the flange of the steel beam. Small wooden blocks, fixed to the sheet pile, served as targets for the horizontal laser displacement measurements. Similarly, PVC panels were attached to the sheet pile as targets for vertical displacement measurements. A separate laser sensor, also mounted on a wooden block and aimed at a small PVC plate located 80 mm behind the sheet pile, measured soil vertical displacement.

Horizontal displacement sensors had a maximum range of 100 mm, while vertical and soil displacement sensors had a range of 50 mm, all with an accuracy of 0.01 mm. Six horizontal displacement sensors were used to measure the out-of-plane horizontal movement of the sheet pile. Two sensors were placed at the edges, and four were positioned within the loading region along the sheet pile (Fig. 4). Four vertical displacement sensors were placed within the loading region along the sheet pile. All laser sensors were connected to a data logger via long cables exceeding 10 m.

The sheet pile's tilt was measured at the top, middle, and bottom of its retained height using triaxial tiltmeters. At the top of the sheet pile, six tiltmeters were installed in close proximity to the horizontal laser displacement measurement locations.

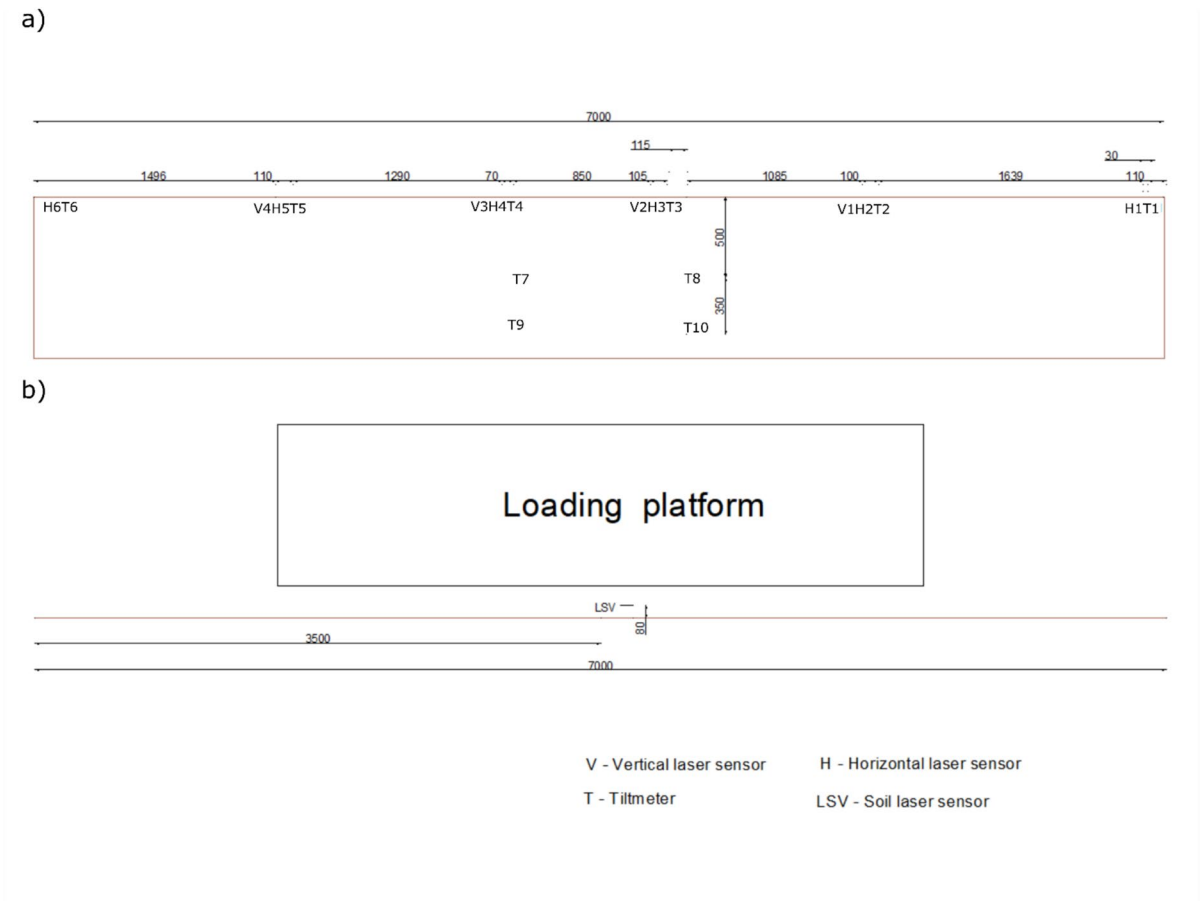


**Fig. 4** Sensor placement on the sheet pile; **a** Elevation/Front view from the canal side, **b** Plan. All dimensions are in mm

At the middle and bottom, tiltmeters were positioned at the longitudinal midsection of the sheet pile.

These tiltmeters were screw-mounted, battery-powered devices employing the LoRaWAN wireless communication protocol. A 230 V-powered gateway, located approximately 10 m from the test area, facilitated real-time data access through the Move Cloud platform. The tiltmeters offered a resolution of 0.000015° and a measurement range of ± 90°.

Data acquisition, including temperature readings, occurred at two-minute intervals throughout the testing period. Synchronization of all ten tiltmeters, strategically placed along the sheet pile, ensured simultaneous tilt data collection.

## 2.5 Spruce Sheet Pile

Following the surcharge loading test, spruce sheet piles were transported to the Biobased Structures and Materials laboratory at Delft University of Technology. Fourteen sheet piles were subjected to four-point flatwise bending tests, conforming to EN 408 (2010), to determine the global modulus of elasticity ($MOE_{s,g}$) and bending strength (MOR). $MOE_{s,g}$ was calculated from mid-span deflection relative to supports. Seven boards were submerged in water for two weeks, before subjecting to four point bending tests, resulting in an average moisture content of 33%, while the remaining seven were tested in air-dry conditions (average moisture content 17%).

Vibration measurements were conducted using Timber grader MTG device manufactured by Brookhuis Micro-Electronics BV. The first mode eigenfrequency was obtained and registered from processing the amplitude time plot using Fast Fourier Transform (FFT), which was displayed real time using the accompanying software of timber grader device. Velocity of the wave was determined as:

$$V = 2L \times f \tag{1}$$

where $L$ is the length of the board in m and $f$ is the first natural frequency in Hz. Using the velocity of the propagating stress wave, the dynamic modulus of elasticity $MOE_{dyn}$ was calculated from the formula:

$$MOE_{\mathrm{dyn}} = V^2 * rho \tag{2}$$

where *rho* is the density.

After completion of four-point bending tests, a representative piece was cut from the tested board. Moisture content (MC %) was determined according to EN 13183-1 (2002).

## 2.6 Modelling Approach and Strategy

This modeling study aimed to evaluate the long-term performance of the bio-engineered solution (softwood timber sheet pile + vegetation) by comparing two distinct stages.

Stage 1 modeled the surcharge loading experiment with spruce sheet pile, representing the initial condition of a bio-engineered solution, where the bank protection consists of only the inert timber material. D-Sheet Piling software was employed for this simulation, and the model was calibrated using horizontal displacement data obtained from the field experiment. D-Sheet Piling is widely adopted by practitioners and researchers in the Netherlands due to its computational efficiency and user-friendly interface (e.g., van Delft 2020; Theunisse 2023).

Stage 2 simulated the combined effects of a decayed spruce sheet pile and vegetation growth ten years post-construction. The natural resistance of wood to decay varies among varied species (EN 350, 2016; Tardio and Mickovski 2023). The biological deterioration along the surface of the wood depends on micro-climatic conditions (the moisture or humidity level of the material's environment), which in turn are influenced by macro-climatic (e.g., rainfall, temperature) and meso-climatic factors (e.g., location, structural details) (Viitanen et al. 2010). The location of the maximum bending moment acting on the timber sheet pile used for bank protection is generally expected to be submerged in water. In such waterlogged environments, biological decay is primarily caused by bacterial activity, which generally has a very low decay rate (Gard et al. 2023; Yang et al. 2025).

Other bio-engineering studies (Tardio and Mickovski 2016, 2023), following the work of Leicester et al. (2003), model wood deterioration as bilinear, where a steady decay is observed after a time lag for decay to begin. In the study on the

deterioration of long-standing timber piles, Yang et al. (2025) used a linear 'fast' decay rate of 0.2 mm/year and a slow decay rate of 0.07 mm/year for spruce. Since no specific data for the decay rate of softwood timber sheet piles is available, a uniform decay rate of 1 mm/year was applied to the spruce sheet pile within the model. To be conservative, no time lag for decay to initiate was included.

To assess the influence of vegetation reinforcement, two separate analyses were conducted, considering the interaction between the decayed sheet pile and the vegetated backfill. Strength increase attributed to Crataegus laevigata DC. root growth, derived from corkscrew extraction experiments in an adjacent plot, were incorporated using both minimal and average measured values. Specifically, the Stage 2 future conditions analyzed were:

- Future scenario 1 (F1): the decayed spruce sheet pile (1 mm/year) without vegetation reinforcement;
- Future scenario 2 (F2): the decayed spruce sheet pile (1 mm/year) with vegetated backfill, using minimal vegetation strength increase; and
- Future scenario 3 (F3): the decayed spruce sheet pile (1 mm/year) with vegetated backfill, using average vegetation strength increase.

F1 represents the reference condition, where the bank protection consists solely of a softwood sheet pile. F2 and F3 represent the evolution of the bio-engineered solution with vegetation and would serve as a comparison to the reference condition to assess any benefits derived from vegetation root reinforcement.

As part of a separate study, corkscrew extraction experiments were performed on *Crataegus laevigata* DC.-rooted soil in a plot approximately 30 m from the current test location (Kamath et al. 2025a). These tests, conducted to a depth of 500 mm, revealed an average strength increase of 16.2 kPa (F3) and a minimal strength increase of 2.3 kPa (F2) for the rooted soils.

This reinforcement effect of roots is commonly represented as an apparent cohesion term, referred to as "root cohesion," which is added to the soil's inherent shear strength and is incorporated into slope stability models (Waldron 1977; Wu et al. 1979; Simon and Collison 2002; Greenwood 2007; Krzeminska et al. 2019; Capobianco et al. 2021). Therefore, in the numerical model, the backfill strength enhancement due to vegetation was represented as an increase in soil cohesion. Given that most roots are concentrated in the upper soil layers, the vegetation reinforcement was incorporated only into the top 0.4-m layer of the model.

## 3 Results and Discussion

### 3.1 Deflection of Sheet Pile

Excavation was performed along the full length of the sheet pile over a period of 40 min. As a result, horizontal displacement was observed to increase during this period, stabilizing thereafter before the commencement of the next step. Horizontal displacement sensors at the sheet pile edges recorded minimal deflection, around 0.25 mm, while central sensors registered a maximum deflection of 0.9 mm (Fig. 5). Vertical displacement sensors showed negligible movement ($<0.2$ mm). The exact cause of the temporary stabilization is unknown but may be a period of stress redistribution and soil arching development, which was subsequently overcome, leading to further settlement. The vertical displacements were nearly zero after the excavation phase concluded, indicating stabilization. The displacement patterns of all horizontal and vertical sensors were similar, albeit with a slight time shift. This shift resulted from the sequential nature of the excavation process, progressing from one end of the sheet pile to the other.

Backfilling to the target retaining height was completed in approximately 45 min. Backfill material was evenly distributed and compacted behind the sheet pile in layers. Following the backfilling procedure, the sheet pile exhibited a maximum horizontal deflection of approximately 3 mm (Fig. 6). This maximum deflection was recorded at the central sensors, H3 and H4. Edge sensors H1 and H6 registered minimal horizontal deflections of approximately 1 mm and 1.2 mm, respectively. All horizontal displacements stabilized after 75 min. Vertical displacements peaked at 0.4 mm upon completion of backfilling. All vertical

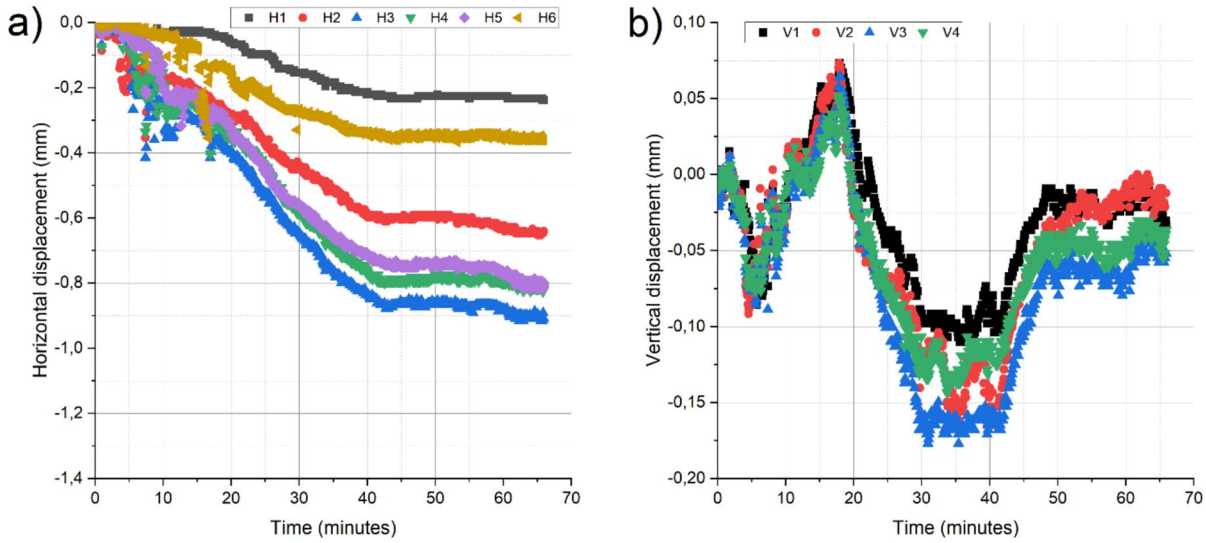


**Fig. 5** Displacement of the sheet pile during excavation recorded at laser sensors **a** horizontal displacement, **b** vertical displacement

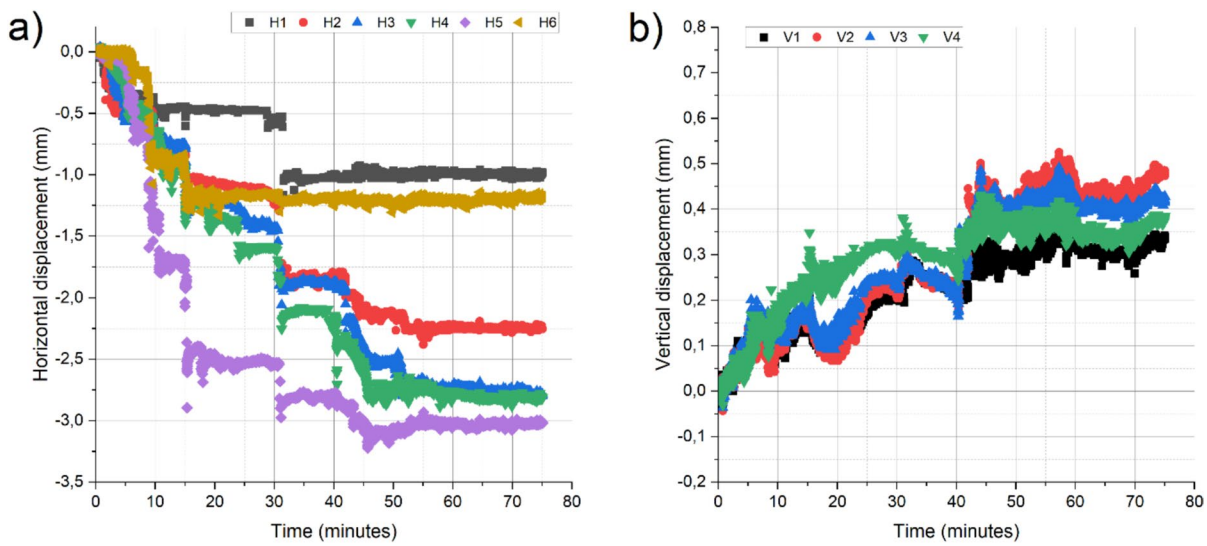


**Fig. 6** Displacement of the sheet pile during backfilling recorded at laser sensors **a** horizontal displacement **b** vertical displacement

displacement sensors displayed a similar pattern, with no significant variation observed between them.

After initiating an artificial rainfall of three hours, a horizontal movement of 0.7 mm was recorded. In case of artificial rainfall as well, the deflection pattern of the sheet pile along the length was similar to that of backfilling and excavation steps. The sensors at centre showed maximum deflection while the edge sensors recorded the minimum deformation of about 0.1 mm (Supplementary material Fig. S1, S2). The vertical displacement of the sheet pile was minimal or averaged to zero during the rainfall for all the three vertical sensors other than V1. Sensor V1 showed values of up to 0.4 mm displacement during the period of rainfall. Since the sensors had to be removed continuous monitoring overnight using the laser sensors was not possible.

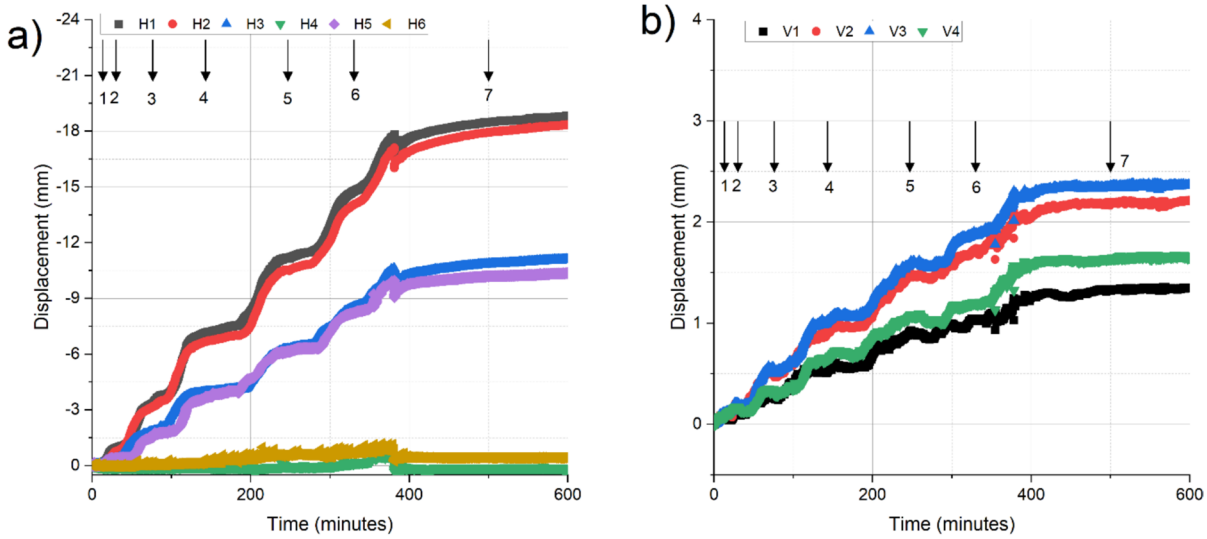


**Fig. 7** Displacement of the sheet pile during surcharge loading recorded at laser sensors **a** Horizontal displacement **b** Vertical displacement. The arrows denote the seven sequential loading stages with approximate surcharge pressures of 2, 5, 10, 15, 20, 25, and 30 kPa

The placement of a steel sheet resulting in a pressure of 1.5 kPa caused a maximum horizontal displacement of 0.1 mm at the centre, as recorded by sensors H3 and H4. At the end of application of 2 kPa load using water tanks, sensors H4 showed a maximum displacement of 0.15 mm and H3 0.12 mm. At the end of 5 kPa loading, the sensors H4 had a deformation of 1 mm and H3 0.79 mm (Fig. 7). After loading to 1/3rd of the maximum planned surcharge loading, i.e.10 kPa, sensors H3 and H4 had a displacement of 3.8 and 3.5 mm, respectively.

Once the rate of change of horizontal displacement was minimum the second layer of tanks were filled to half resulting in surcharge loading of 15 kPa. At 15 kPa surcharge load the sheet pile at the centre moved by H3 7.5 mm and H4 by 7 mm, respectively. On filling the second layer of tanks, resulting in 20 kPa loading, the displacement at the centre increased to 11.5 mm and 10.8 mm. When the third layer of tanks were filled to half a loading of 25 kPa was applied, sheet pile movement of 15 and 14 mm were recorded at the centre. Finally, after filling all the three layers of tanks a displacement of 18.2 mm and 17.6 mm was recorded. After leaving the load overnight a maximum displacement of 19.3 and 18.8 mm was recorded. The pattern of displacement of the sheet pile along the length was consistent for all surcharge loads applied. In all the loads applied, the edges of the sheet pile (H1 and H6) showed least displacement, followed by H2 and H5.

All the vertical displacement sensors showed a downwards movement and similar trend with each loading step. Vertical sensors V2 and V3, showed higher displacements than V1 and V4 which were placed towards the edge of the loading area. A soil settlement of about 32 mm was observed at the end of the surcharge loading (Fig. 8). The settlement corresponds to 3.2% of the retaining height.

There has been considerable experimental and numerical study on the response of pile walls to surcharge loading (Georgiadis and Anagnostopoulos 1998; Singh and Chatterjee 2020; Mishra and Sawant 2023; Debnath et al. 2024). However, most of these studies rely on either laboratory-scale models or sheet piles made from materials other than softwood, which makes a direct comparison with the present results challenging.

Aparna and Samadhiya (2019) observed that maximum settlement was observed when the surcharge load (in their case a footing placed at surface) was placed closer to the wall and within the Rankine's wedge. The lateral soil displacement with the movement of the sheet pile also contribute to the heightened settlement of the footing when placed

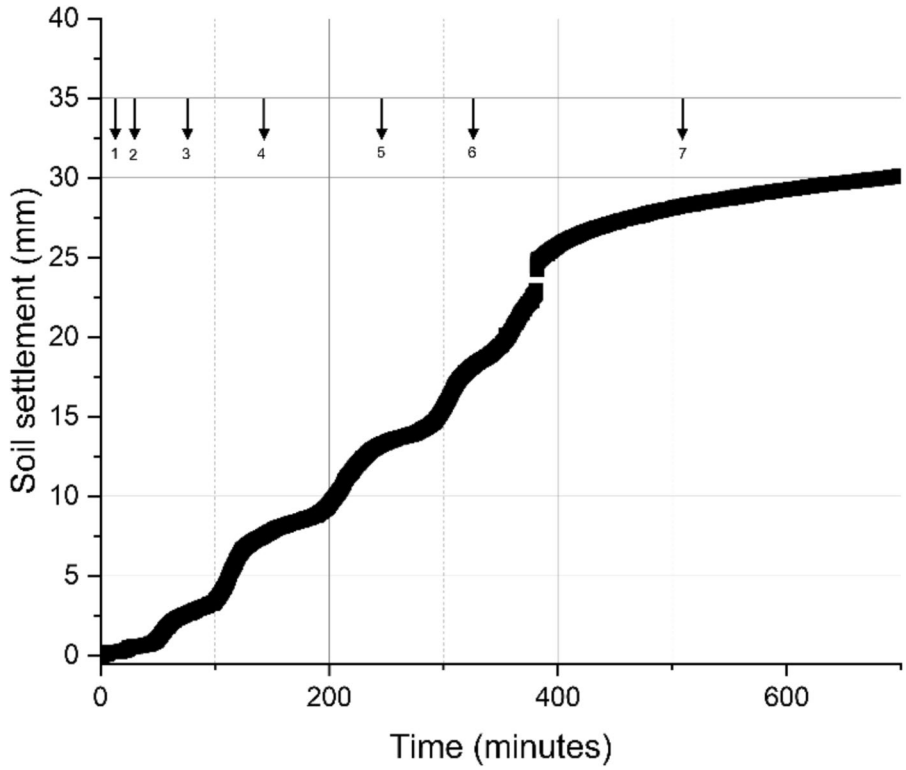


**Fig. 8** Soil settlement at the backfill during the surcharge loading. The arrows denote the seven sequential loading stages with approximate surcharge pressures of 2, 5, 10, 15, 20, 25, and 30 kPa

in proximity to the excavation face (Aparna and Samadhiya 2019).

Construction of wooden sheet pile canal bank barriers is classified under Safety Class 1 according to CUR 166. While CUR 166 does not specify maximum deflection requirements for wooden sheet piles, it does provide guidelines for steel sheet piles. In this study, we adopted the steel sheet pile deflection criterion, which assumes a maximum allowable deflection of 1/100 of the retaining height, for the wooden sheet piles. Based on this criterion, the surcharge experiment resulted in a deflection of approximately 1.9% of the retaining height, exceeding the allowable deflection criterion.

Non-linear increase in displacement with surcharge loading for cantilever sheet piles was reported by Aparna and Samadhiya (2019) and Rauf et al. (2021). Madabhushi and Chandrasekaran (2005) showed that excessive displacement of the cantilever sheet pile is observed as the shear demand reaches the maximum strength of the backfill material. Such a sudden increase in displacement of the sheet pile was also observed on 1 g tests on cantilever sheet pile walls subjected to surcharge loading (Rauf et al. 2021) The increase in displacement was seen to increase with applied *g*-level in centrifuge tests (Madabhushi and Chandrasekaran 2005).

Application of the full 30 kPa surcharge load resulted in the formation of cracks (Fig. 9), extending along a four-meter section within the loaded area. Although the depth of these cracks remained undetermined, visual inspection indicated they were not superficial. The longer edge of the steel sheet, adjacent to the sheet pile, settled 110 mm by the end of the test. Based on a soil unit weight of 16.6 to 17.5 kN/m$^3$, the theoretical failure plane may intersect the backfill surface at 1.26 m to 1.31 m from the sheet pile wall. The observed crack location was approximately 1.25 m from the wall.

### 3.2 Tilt of the Sheet Pile

During excavation phase, slightly different tilts were measured at both edges of the sheet piles. As expected, the tilt measured at the edges of the sheet pile was least (T6). T3 recorded the highest tilt during excavation phase. The tilt sensors at mid depth of the


**Fig. 9** Initiation of cracks **a** Cracks running full length behind loading, **b** Close up view of cracks

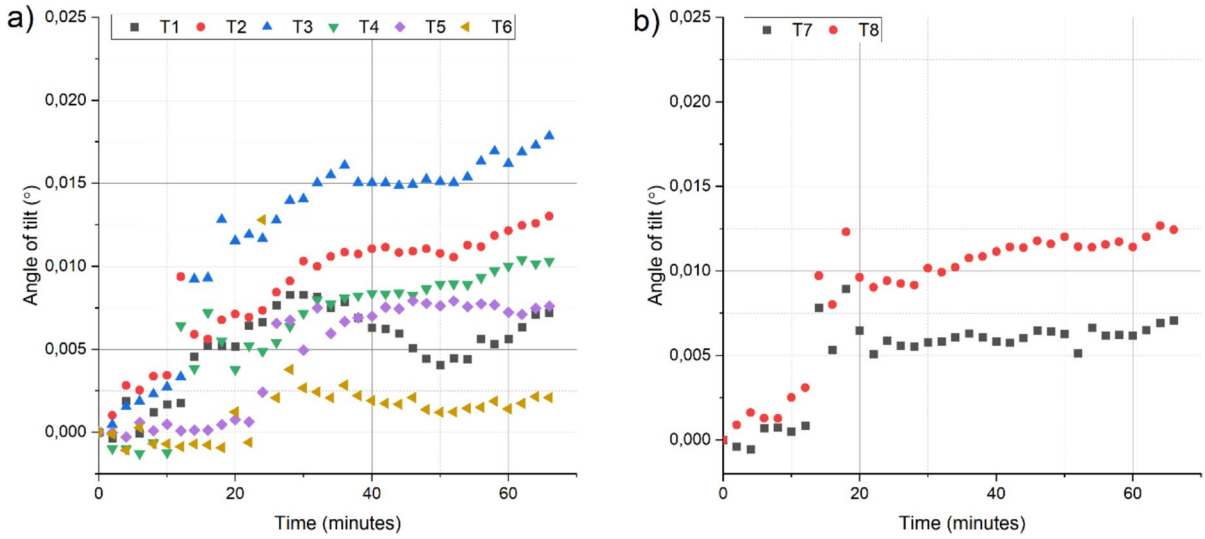


**Fig. 10** Tilt of the sheet pile during excavation **a** Tiltmeters T1-T6, **b** Tiltmeters T7-T8

sheet pile: T7, T8 also showed similar tilt angles as tilt sensors T3 and T4 respectively (Fig. 10).

T5 showed highest tilt measurements after the backfill procedure (0.12°), followed by T4 and T3 tiltmeters (Fig. 11). Similar response is shown in the deflection measurements, confirming the coherent response behaviour of both the tilt and displacement sensors. Tiltmeters at either edge showed the least tilt during backfilling. Tiltmeters T7, T8, T9, T10 showed same trend during backfilling procedure and had similar values with the corresponding tiltmeter on the top.

The tilt readings during loading clearly shows the maximum tilt at the centre which reduces to minimum at the edges of the sheet pile. At 10 kPa loading tilt measured at sensors T3 and T4 was 0.14°

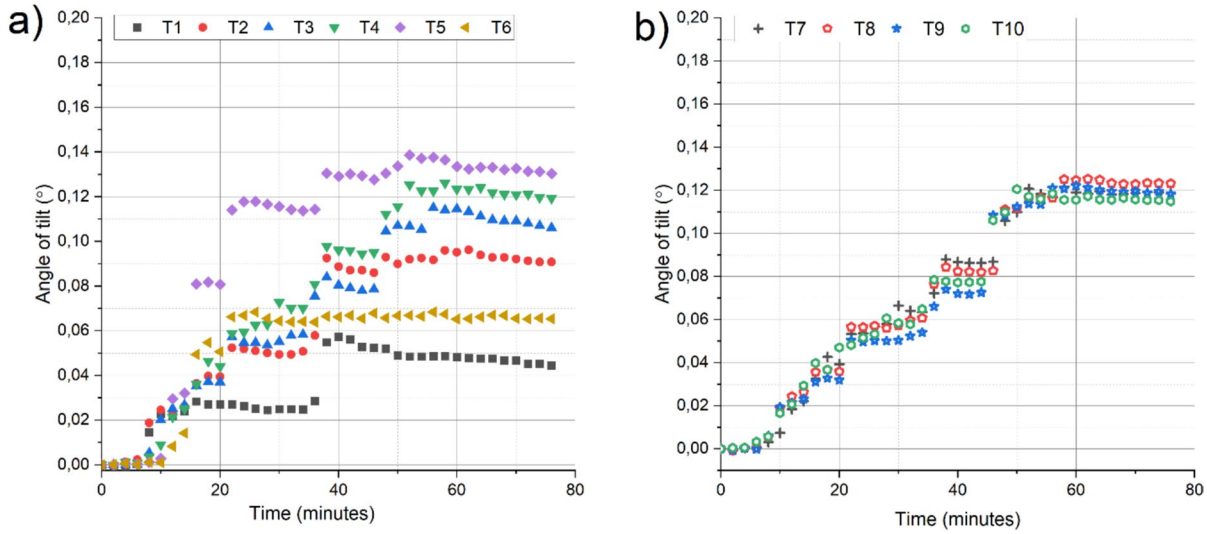


**Fig. 11** Tilt of the sheet pile during backfilling **a** Tiltmeters T1-T6, **b** Tiltmeters T7-T10

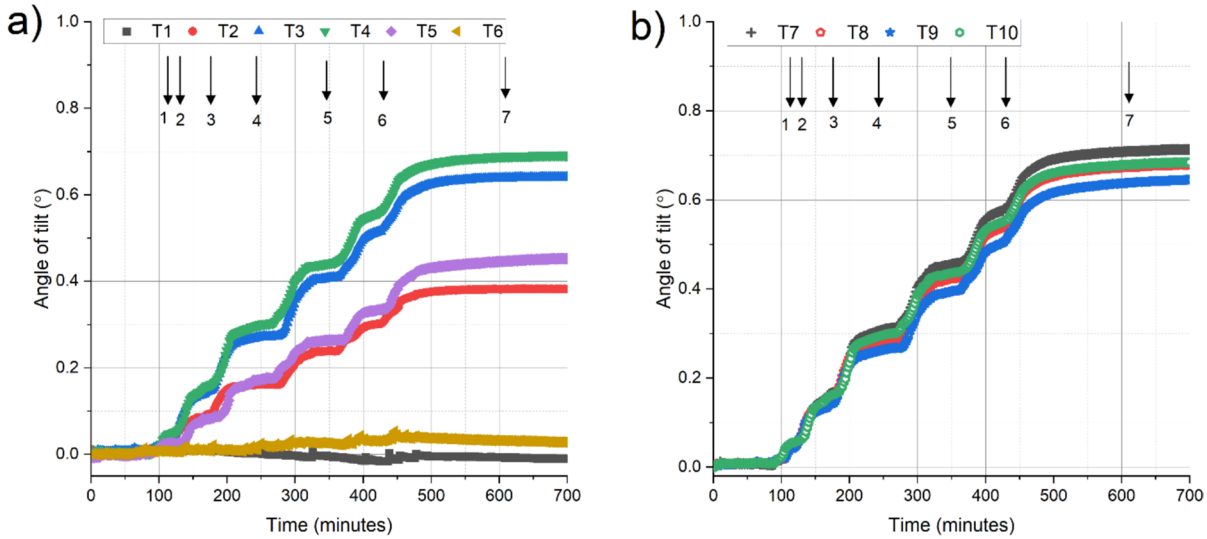


**Fig. 12** Tilt of the sheet pile during loading **a** Tiltmeters T1-T6, **b** Tiltmeters T7, T8, T9, T10

and 0.15° (Fig. 12). The tilt angles of T3 and T4 increased to 0.40° and 0.44° respectively at 20 kPa loading and further increased to 0.62° and 0.67° respectively at 30 kPa loading. The tilt angles measured at full loading at sensors T7, T8, T9, T10 were 0.71°, 0.68°, 0.64° and 0.68° respectively.

The average tiltmeter values at the end of the experiment—0.664° at the top, 0.709° at mid-depth, and 0.687° at the bottom—reveal a nonlinear tilt profile characterized by peak curvature at mid-depth and reduced rotation near the toe of excavation. This pattern is broadly consistent with the flexural bending response typically expected in embedded retaining walls, where maximum curvature develops around mid-height while toe movements are restrained by embedment. Numerical integration of the tilt angles, segmented into four sections with linear interpolation, yields a rotational displacement

contribution of ~ 12.3 mm at the top. This falls short of the measured 19.05 mm, leaving a residual displacement of ~ 6.7 mm, potentially due to toe translation and kick-in effects associated with vertical settlement. The nonlinear tilt distribution therefore underscores bending-dominated wall behaviour, while the residual displacement indicates coupled bending–translation mechanisms, both of which align with known responses of flexible retaining systems under surcharge loading. Traditional rigid-rotation models may underestimate displacements, highlighting the need for advanced numerical tools (e.g., D-Sheet Piling) or field-calibrated tilt data to capture these coupled effects.

Hemel (2023) proposed incorporating prism measurements along with tilt sensors on the gravity wall as part of a monitoring strategy to detect potential lateral failures of quay walls in Amsterdam's city center. In the Netherlands and worldwide, with aging infrastructures such as quay walls, large interest is shown in monitoring and predicting the current state of such structures using distinct types of sensors with inclination measurements e.g. Smart brick project from Althen sensors BV.

### 3.3 Spruce Boards

The mechanical properties obtained for the tested spruce sheet piles are presented in Table 2. The global modulus of elasticity ($MOE_{s,g}$) was further adjusted to a reference 12% moisture content according to the guidelines provided in EN 384:2016 + A2:2022. The average $MOE_{s,g}$ at reference moisture content ($MOE_{s,g12}$) for the air-dry boards was 8500 MPa, while the average $MOE_{s,g12}$ for the wet boards was 7100 MPa. Practicing engineers commonly utilize the local modulus of elasticity ($MOE_{s,l}$), which represents the modulus of elasticity in pure bending, for design calculations.

Ravenshorst (2005), based on their testing of a large number of European softwood samples including spruce, found a correlation between $MOE_{s,l}$ and $MOE_{s,g}$ expressed as: $MOE_{s,l} = 1.11 \times MOE_{s,g}$ with a coefficient of determination ($R^2$) of 0.78. $MOE_{s,l}$ at reference moisture conditions for the boards tested in air-dry based on the above corelation is 9500 MPa and that of boards tested in wet condition 7900 MPa.

### 3.4 Modelling

The surcharge loading experiment was modelled in D-sheet piling with the obtained spruce sheet pile and soil parameters. A wall friction of 2/3* friction angle was assumed. Soil density corresponding to Table 1 was given to different layers. The first step was to calibrate the model to match the experimentally obtained horizontal displacement during surcharge loading. The parameters of soil friction angle and elastic stiffness was fine tuned to match the displacement of the sheet pile during surcharge loading recorded by laser sensors at the middle of the section, H3 and H4. The parameters that best match the experimentally obtained displacement are given in Table 3.

Following the calibration procedure, a uniform soil friction angle (ϕ), 41° and elastic stiffness (EI) of 240 $kNm^2/m'$ was seen to best represent the horizontal

**Table 3** Input parameters for D-sheet pile model for calibration and future scenarios

| Parameter | Value | Units |
|---|---|---|
| Depth of sheet pile | 2.3 | m |
| Elastic stiffness (EI) calibration | 240 | $kNm^2/m'$ |
| Elastic stiffness (EI) (F1, F2, F3) | 145 | $kNm^2/m'$ |
| Soil friction angle (ϕ) | 41 | 0 |
| Root cohesion (F2) | 2.3 | kPa |
| Root cohesion (F3) | 16.2 | kPa |

**Table 2** Average mechanical properties of spruce timber sheet pile from four point bending tests

| | No | Width (mm) | Length (mm) | Thickness (mm) | Density ($kg/m^3$) | MC (%) | $MOE_{dyn}$ (MPa) | MOR (MPa) | $MOE_{s,g}$ (MPa) |
|---|---|---|---|---|---|---|---|---|---|
| Dry | 7 | 203 | 2300 | 65 | 447 | 16.9 | 10,500 | 34.8 | 8100 |
| Wet | 7 | 203 | 1700 | 65 | 543 | 33.2 | 9600 | 32.1 | 6600 |

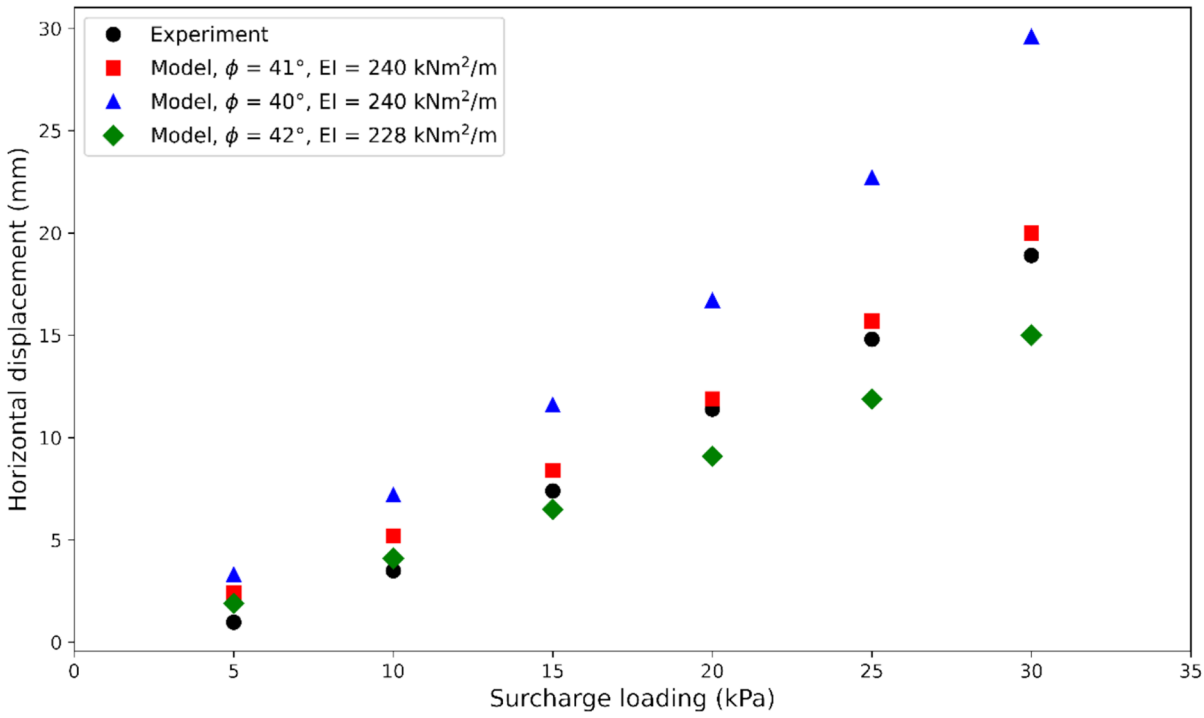


**Fig. 13** Validation of the numerical model: Horizontal displacement of the sheet pile under increasing surcharge loading, comparing experimental measurements with simulations using different friction angle (ϕ) and pile elastic stiffness (EI) parameters

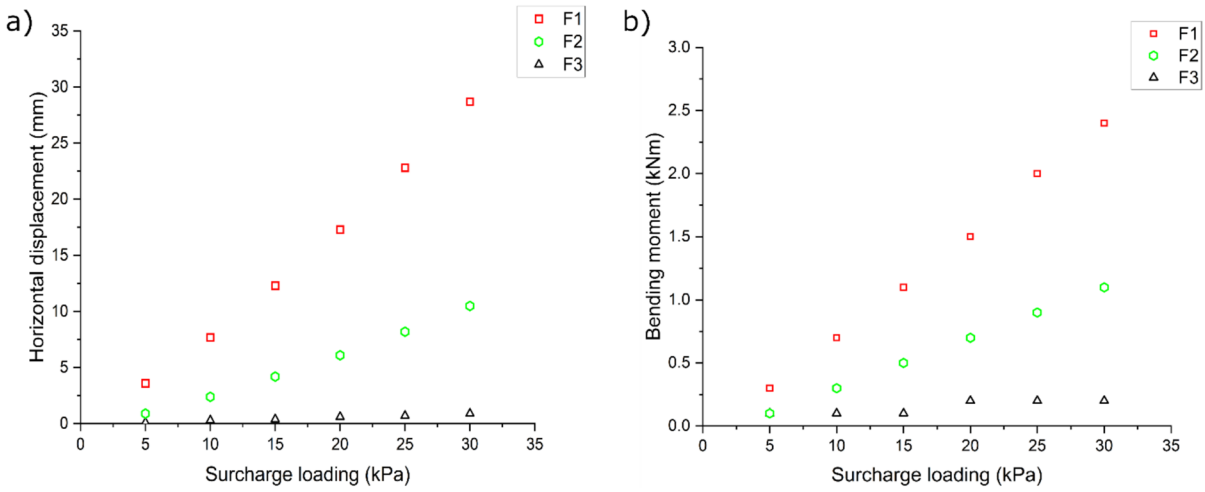


**Fig. 14** **a** Horizontal displacement (mm) and **b** additional bending moment (kNm) of the sheet pile under increasing surcharge loading (kPa) for different future scenario's (F1, F2, and F3)

displacement obtained from the surcharge test, see Fig. 13. On calibration additional bending moment of 2.4 kNm and shear force of 5.8 kN was obtained to be acting on the sheet pile at the end of the surcharge loading. The total bending moment acting on the sheet pile (6 kNm) will result in a relatively low bending stress when compared to average bending strength obtained from four point bending tests (< 50%).

Using the calibrated model, future scenario, as given in Sect. 2.3, was modelled next. F1 future scenario results in horizontal displacement of 28.7 mm of the spruce sheet pile after 10 years of service see Fig. 14a. This would represent a displacement of 2.8% of the retaining height which can be expected when a uniform decay of 1 mm/year of the spruce sheet pile is taken. The displacement reduces to 10.5 mm in scenario F2 and 0.9 mm in scenario F3 when full surcharge loading is applied. Similarly, additional bending moment acting on the sheet pile also reduces from 2.4 to 1.1 kNm in future scenario F2. The additional bending moment reduces to nearly zero, (0.2kNm), when maximum vegetation reinforcement has developed in time, see Fig. 14b.

This study assumes a relatively high decay rate with no initial time lag for decay, which constitutes a conservative approach. While data on hardwood timber decay is available (Kamath et al. 2025b), there is little information on the decay of softwood sheet piles in service. Consequently, the assumed decay rate used in this study should be interpreted with caution. To address this knowledge gap, field-scale monitoring studies are currently underway at the same test location to measure the actual deterioration of softwood timber sheet piles.

While modelling root reinforcement in slope stability analysis, majority of the studies assume a uniform cohesion in the rooted zone (Switala and Wu 2015; Krzeminska et al. 2019; Aziz and Islam 2022). As suggested by Murgia et al. (2022), this assumption is made because of lack spatially explicit data regarding root reinforcement density or depth. However, spatial variability of root reinforcement can occur within the root zone in the bank. Overlooking, this spatial variability of root reinforcement can result in overestimation of contribution of roots to stability. This study used the corkscrew extraction technique to estimate root reinforcement, which helped to better define the depth of the root zone and range of root reinforcement. However, applying this reinforcement uniformly across the entire root zone depth has the limitations previously outlined.

There is little data available on monitoring of performance of bio-engineered bank retaining structures involving timber and vegetation combinations. However, indications of the influence of vegetation on deformation characteristics of soil slopes is documented in studies from Switala and Wu 2015 and Liang et al. (2020). Uniformly distributed vegetation reinforcement, as assumed in this study, was found to have highest values of factor of safety for sandy slopes (Switala and Wu 2015). In presence of rooted zones, reduction in crest settlement on sandy slope of short heights were reported when subjected to earthquake loading (Liang et al. 2020). Hu et al. (2013) reported higher soil cohesion for rooted samples and an associated restraining effect and reduction in lateral deformation compared to fallow soils. The abovementioned reinforces our findings that a reduction in lateral displacement of the decayed sheet pile can be expected when the backfill has vegetation root reinforcement.

## 4 Conclusion

The full-scale field surcharge loading test on spruce timber sheet piles and consequent numerical modeling successfully evaluated the feasibility of using locally available wood with vegetation as a nature-based solution for canal bank protection. Excavation and backfilling of approximately 10% of the retaining height resulted in displacements of less than 1 mm (0.1% of retaining height) and about 3 mm (0.3% of retaining height), respectively.

Under the applied 30 kPa surcharge load, the sheet pile wall exhibited a horizontal displacement of 18.9 mm (1.9% of retaining height) and a corresponding soil settlement of 32.9 mm. The wall's tilt profile (0.66° top, 0.71° mid, 0.69° bottom) demonstrated bending dominance, with peak curvature at mid-depth, signifying flexural deformation rather than rigid rotation. The total deformation exceeded the permissible limits for permanent sheet piles as specified by CUR 166 guidelines.

Simulations for a 10-year period, including anticipated material decay, showed that a decayed spruce sheet pile would experience a significant maximum horizontal displacement of 28.7 mm under surcharge loading. However, when root reinforcement from *Crataegus laevigata* DC was included in the model, displacements were substantially reduced to 10.5 mm (minimum root reinforcement) and 0.9 mm (average root reinforcement). The root reinforced backfill also decreased the additional bending moment on the sheet pile from 2.4 to 1.1

kNm under surcharge loading, demonstrating the significant stabilizing effect of this bio-engineered approach.

**Acknowledgements** The authors gratefully acknowledge the *Provincie Noord-Holland* for having funded the research study and provided the test site and analyzed wooden sheet piles.

**Funding** Abhijith Kamath reports financial support was provided by Provincie Noord-Holland. If there are other authors, they declare that they have no known competing financial interests or personal relationships that could have appeared to influence the work reported in this paper.

**Data availability** Data supporting the findings of this study are available from the corresponding author upon reasonable request.

**Declarations**

**Conflict of interest** The authors declare that there is no conflict of interest.



## References

Acharya MS (2018) Analytical approach to design vegetative crib walls. Geotech Geol Eng 36(1):483–496

Ali FH, Osman N (2008) Shear strength of a soil containing vegetation roots. Soils Found 48(4):587–596

Andreoli A, Chiaradia EA, Cislaghi A, Bischetti GB, Comiti F (2020) Roots reinforcement by riparian trees in restored rivers. Geomorphology 370:107389

Aparna, Samadhiya NK (2019) Evaluation of model sheet pile wall adjacent to a strip footing: an experimental investigation. Int J Geotech Eng 14(7):828–835

Aziz S, Islam MS (2022) Mechanical effect of vetiver grass root for stabilization of natural and terraced hill slope. Geotech Geol Eng 40(6):3267–3286

Bigham KA (2020) Streambank stabilization design, research, and monitoring: the current state and future needs. Trans ASABE 63(2):351–387

Böll A, Burri K, Gerber W, Graf F (2009) Long-term studies of joint technical and biological measures. For Snow Landsc Res 82(1):9–32

Capobianco V, Robinson K, Kalsnes B, Ekeheien C, Høydal Ø (2021) Hydro-mechanical effects of several riparian vegetation combinations on the streambank stability—a benchmark case in southeastern Norway. Sustainability 13(7):4046

CUR (Civieltechnisch Centrum Uitvoering en Regelgeving) (1994) CUR 166: Damwandconstructies. CUR, Gouda

Debnath A, Pal SK (2023) Influence of surcharge strip loads on the behavior of cantilever sheet pile walls: a numerical study. J Eng Res 11(1):100029

Debnath A, Debnath S, Pal SK (2024) Behaviour of sheet pile wall on sloping ground for strip footing as surcharge with coir geotextile reinforced backfill soil. Multiscale Multidiscip Model Exp des 7(6):5429–5443

van Delft V (2020) Global buckling mechanism of sheet piles: The influence of soil to the global buckling behaviour of sheet piles

Deltares (2024) D-sheet piling. Retrieved from deltares: https://www.deltares.nl/softwareen-data/producten/d-sheet-piling

Dias ASRA (2019) The effect of vegetation on slope stability of shallow pyroclastic soil covers (Doctoral dissertation, Université Montpellier; Università degli studi di Napoli Federico II. Istituto di fisica).

EN 350 (2016) Durability of wood and wood-based products—testing and classification of the durability to biological agents of wood and wood-based materials. European Committee for Standardization, Brussels

EN 384:2016+A1:2018. Structural timber. Determination of characteristic values of mechanical properties and density. European Committee of Standardization (CEN), Brussels, Belgium. Released 2019-03-13 as UNE-EN384:2016+A1:2019.

EN 13183-1:2002. Moisture content of a piece of sawn timber. Part 1: Determination by oven dry method. European Committee of Standardization (CEN), Brussels, Belgium. Released 2002-07-29 as UNE-EN 13183-1:2002

Evette A, Labonne S, Rey F, Liebault F, Jancke O, Girel J (2009) History of bioengineering techniques for erosion control in rivers in Western Europe. Environ Manag 43(6):972–984

Fernandes JP, Guiomar N (2016) Simulating the stabilization effect of soil bioengineering interventions in Mediterranean environments using limit equilibrium stability models and combinations of plant species. Ecol Eng 88:122–142

Gard W, Ravenshorst G, van de Kuilen JW (2023) Historical wooden pile foundations in Amsterdam: an integrated approach for the estimation of structural performance and residual service life. In International conference structure anal. Hist. Constr. Springer Nature Switzerland, Cham, pp 1370–1382

Georgiadis M, Anagnostopoulos C (1998) Lateral pressure on sheet pile walls due to strip load. J Geotech Geoenviron Eng 124(1):95–98

Gopal Madabhushi SP, Chandrasekaran VS (2005) Rotation of cantilever sheet pile walls. J Geotech Geoenviron Eng 131(2):202–212

Gray DH, Sotir RB (1996) Biotechnical and soil bioengineering slope stabilization: a practical guide for erosion control. Wiley

Greenwood JR (2007) SLIP4EX–a program for routine slope stability analysis to include the effects of vegetation, reinforcement and hydrological changes. In Eco- and ground bio-engineering: the use of vegetation to improve slope stability: proceedings of first international conference eco-eng. 13–17 September 2004. Springer Netherlands, Dordrecht, pp 193–202

Guo M, Wang W, Shi Q, Chen T, Kang H, Li J (2019) An experimental study on the effects of grass root density on gully headcut erosion in the gully region of China's Loess Plateau. Land Degrad Dev 30(17):2107–2125

Hemel M (2023) Amsterdam quays under pressure: modelling and testing of historic canal walls. Technische Universiteit Delft, Delft

Hu XS, Brierley G, Zhu HL, Li GR, Fu JT, Mao XQ, Qiao N (2013) An exploratory analysis of vegetation strategies to reduce shallow landslide activity on loess hillslopes, Northeast Qinghai-Tibet Plateau, China. J Mt Sci 10:668–686

Hubble T, Clarke S, Stokes A, Phillips C (2017) 4th international conference on soil bio-and eco-engineering (SBEE2016) 'The Use of Vegetation to Improve Slope Stability'. Ecol Eng 109: 141–144

Jiang X, Qian Y, Yang H, Xiao Z, Fan W, Zhu Y, Liu W, Guo J (2022) Model test studies on slope supported by bamboo anchor and timber frame beam. Geotech Geol Eng 40(9):4327–4344

Kamath A, van Bergen K, Ravenshorst G, van de Kuilen W (2025a) Assessment of canal bank stability with vegetation root reinforcement. Ecol Eng 217:107623. https://doi.org/10.1016/j.ecoleng.2025.107623

Kamath A, Kumar GSRKS, Ravenshorst G, van de Kuilen J (2025b) Mechanical strength characterization of recovered azobé timber boards for reuse. Case Stud Constr Mater 22:e04228. https://doi.org/10.1016/j.cscm.2025.e04228

Krymer V, Robert A (2014) Stream restoration and cribwall performance: a case study of cribwall monitoring in southern Ontario. River Res Appl 30(7):865–873

Krzeminska D, Kerkhof T, Skaalsveen K, Stolte J (2019) Effect of riparian vegetation on stream bank stability in small agricultural catchments. CATENA 172:87–96

Li YF, Chen CK, Chen W (2021) Case study of GFRP as a sheet-pile wall for stream bank protection in Taiwan. Case Stud Constr Mater 15:e00602

Li Z, Wang M, Yu S, Liu J (2024) Effects of the root's distribution on the stability of slope. Geotech Geol Eng 42(2):1009–1019

Liang T, Knappett JA, Leung AK, Bengough AG (2020) Modelling the seismic performance of root-reinforced slopes using the finite-element method. Geotech 70(5):375–391

Mickovski SB, Gonzalez-Ollauri A, Sorolla A, Löchner A, Emmanuel R (2024) A case history of co-design and co-deployment of a nature-based solution (NbS) against erosion and slope instability. Ecol Eng 209:107406

Mishra A, Sawant VA (2023) A detailed investigation on contiguous pile wall with homogeneous backfill. Geotech Geol Eng 41(3):2065–2089

Murgia I, Giadrossich F, Mao Z, Cohen D, Capra GF, Schwarz M (2022) Modeling shallow landslides and root reinforcement: a review. Ecol Eng 181:106671

NEN-EN-408 (2010) Timber structures—structural timber and glued laminated timber—determination of some physical and mechanical properties. Nederlands Normalisatie-instituut, Delft, The Netherlands

Ni JJ, Leung AK, Ng CWW, Shao W (2018) Modelling hydro-mechanical reinforcements of plants to slope stability. Comput Geotech 95:99–109

Pollen-Bankhead N, Simon A (2010) Hydrologic and hydraulic effects of riparian root networks on streambank stability: is mechanical root-reinforcement the whole story? Geomorphology 116(3–4):353–362

Rauf I, Hrianto T, Kusnadi K (2021) Laboratorium experimental of cantilever sheet pile behaviour on soft soil induced by strip load. In E3S Web conference, vol 328, p 10020. EDP Sciences

Ravenshorst GJP (2015) Species independent strength grading of structural timber. Technische Universiteit Delft, Delft

Simon A, Collison AJ (2002) Quantifying the mechanical and hydrologic effects of riparian vegetation on streambank stability. Earth Surf Process Landf 27(5):527–546

Singh AP, Chatterjee K (2020) Ground settlement and deflection response of cantilever sheet pile wall subjected to surcharge loading. Indian Geotech J 50(4):540–549

Stokes A, Douglas GB, Fourcaud T, Giadrossich F, Gillies C, Hubble T, Kim JH, Loades KW, Mao Z, McIvor IR, Mickovski SB, Mitchell S, Osman N, Phillips C, Poesen J, Polster D, Preti F, Raymond P, Rey F, Schwarz M, Walker LR (2014) Ecological mitigation of hillslope instability: ten key issues facing researchers and practitioners. Plant Soil 377(1):1–23

Switala BM, Wu W (2015) Numerical simulations of the mechanical contribution of the plant roots to slope stability. Recent Adv Model Landslides Debris Flows, pp 265–274

Tardío G, Mickovski SB (2016) Implementation of eco-engineering design into existing slope stability design practices. Ecol Eng 92:138–147

Tardio G, Mickovski SB (2023) A novel integrated design methodology for nature-based solutions and soil and water bioengineering interventions: the Tardio&Mickovski methodology. Sustainability 15(4):3044

Theunisse A (2023) Comparison of design methods for quay walls: Based on measured deformations in Eemshaven Groningen

Van de Kuilen JWG, Blaß HJ (2005) Mechanical properties of azobé (*Lophira alata*). Holz Roh Werkst 63:1–10

Viitanen H, Toratti T, Makkonen L, Peuhkuri R, Ojanen T, Ruokolainen L, Räisänen J (2010) Towards modelling of decay risk of wooden materials. Eur J Wood Wood Prod 68(3):303–313

Waldron LJ (1977) The shear resistance of root-permeated homogeneous and stratified soil. Soil Sci Soc Am J 41(5):843–849

Wu TH, McKinnell WP III, Swanston DN (1979) Strength of tree roots and landslides on Prince of Wales Island. Alaska Can Geotech J 16(1):19–33

Yang C, Khaloian-Sarnaghi A, Yu T, van de Kuilen JW (2025) A numerical method to integrate duration-of-load and

bacterial deterioration for long-standing timber piles. Wood Sci Technol 59(3):1–15

Zhang D, Cheng J, Liu Y, Zhang H, Ma L, Mei X, Sun Y (2018) Spatio-temporal dynamic architecture of living brush mattress: root system and soil shear strength in riverbanks. Forests 9(8):493